© 2022. This manuscript version is made available under the CC-BY-NC-ND 4.0 license https://creativecommons.org/licenses/by-nc-nd/4.0/

Supplementary Figures:

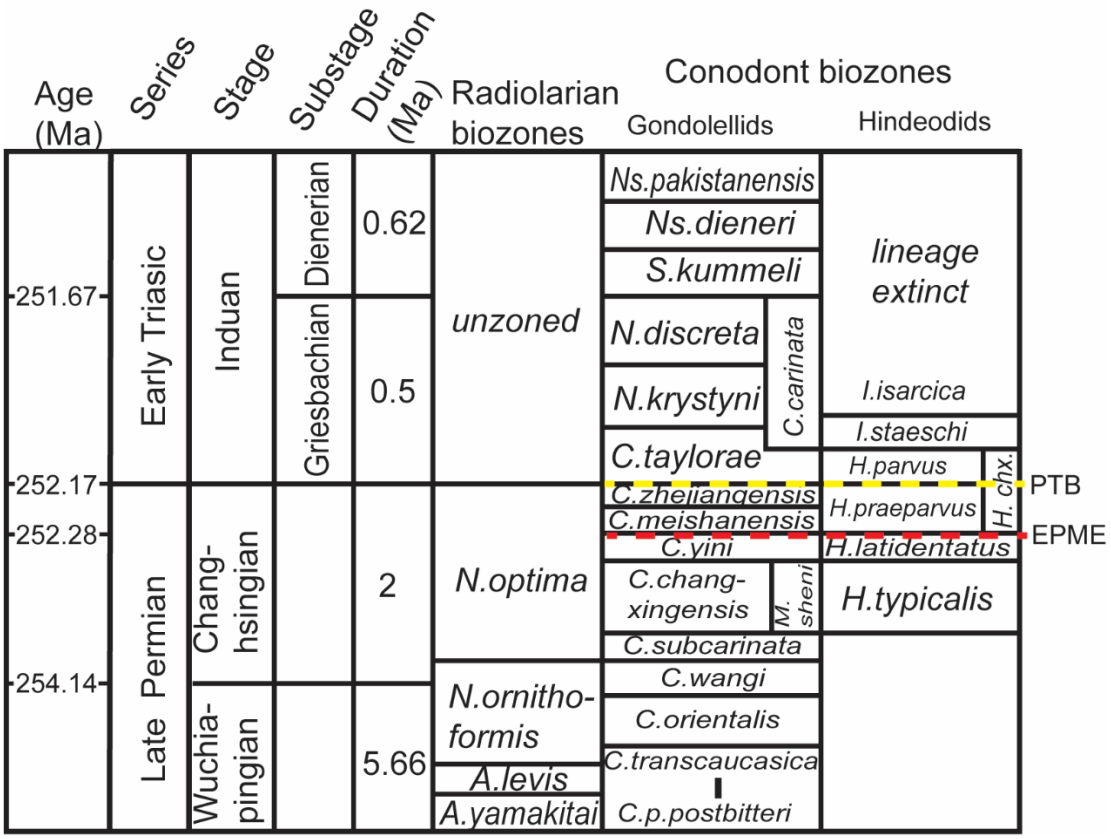

Fig. S1 Typical conodont zone division in the Permian-Triassic boundary interval in the South China (Modified from Shen et al., 2015). Abbreviations: radiolarian genera: A. = Albaillella, E. = Eptingium, N. = Neoalbaillella; Conodont genera: C. = Clarkina, H. = Hindeodus, I. = Isarcicella, N. = Neoclarkina., chx. = changxingensis.

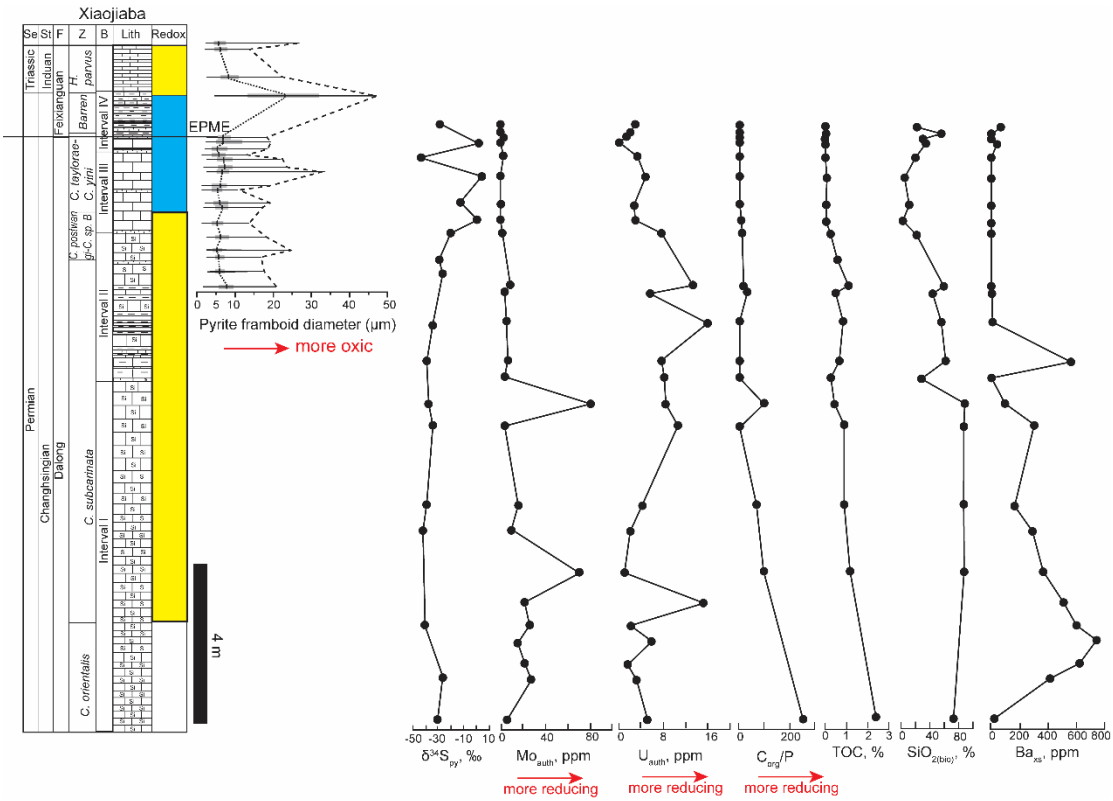

Fig. S2 Lithology, redox and redox-related proxies (indicated by red arrows), productivity proxies (TOC, $SiO_{2(bio)}$, and Ba_{xs}) in the Xiaojiaba section. Details of data and related explanation can be seen in Wei et al. (2015).

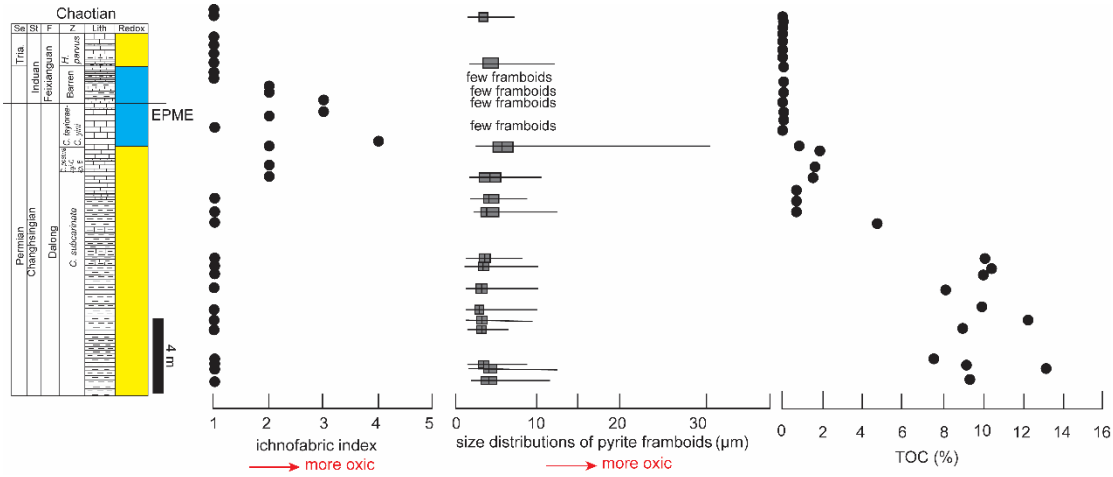

Fig. S3 Lithology, redox and redox-related proxies in the Chaotian section. Details of data and related explanation can be seen in Saitoh et al. (2021).

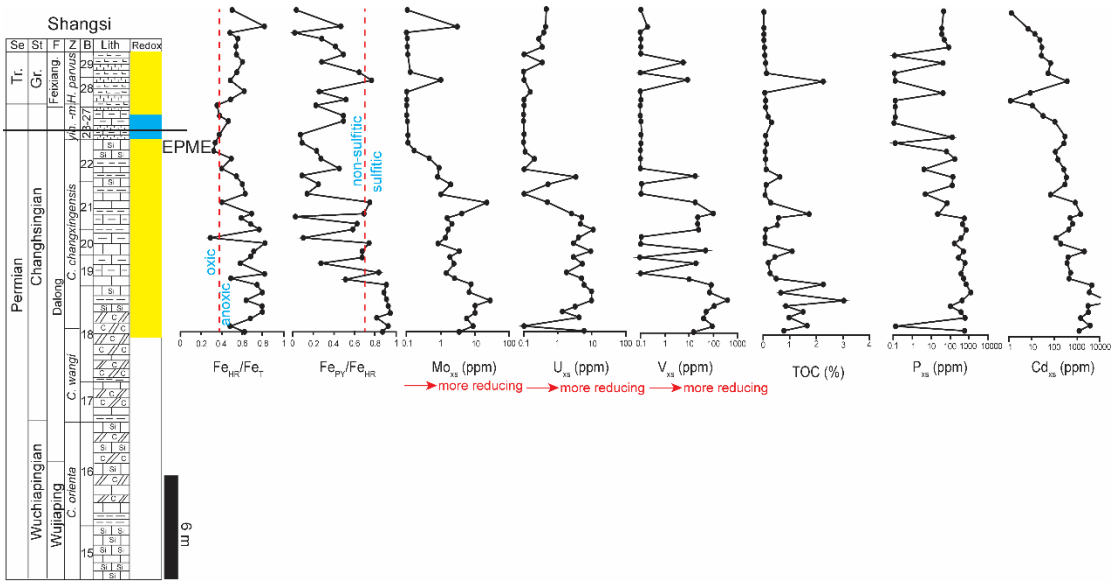

Fig. S4 Lithology, redox and redox-related proxies in the Shangsi section. Details of data and related explanation can be seen in Xiang et al. (2016).

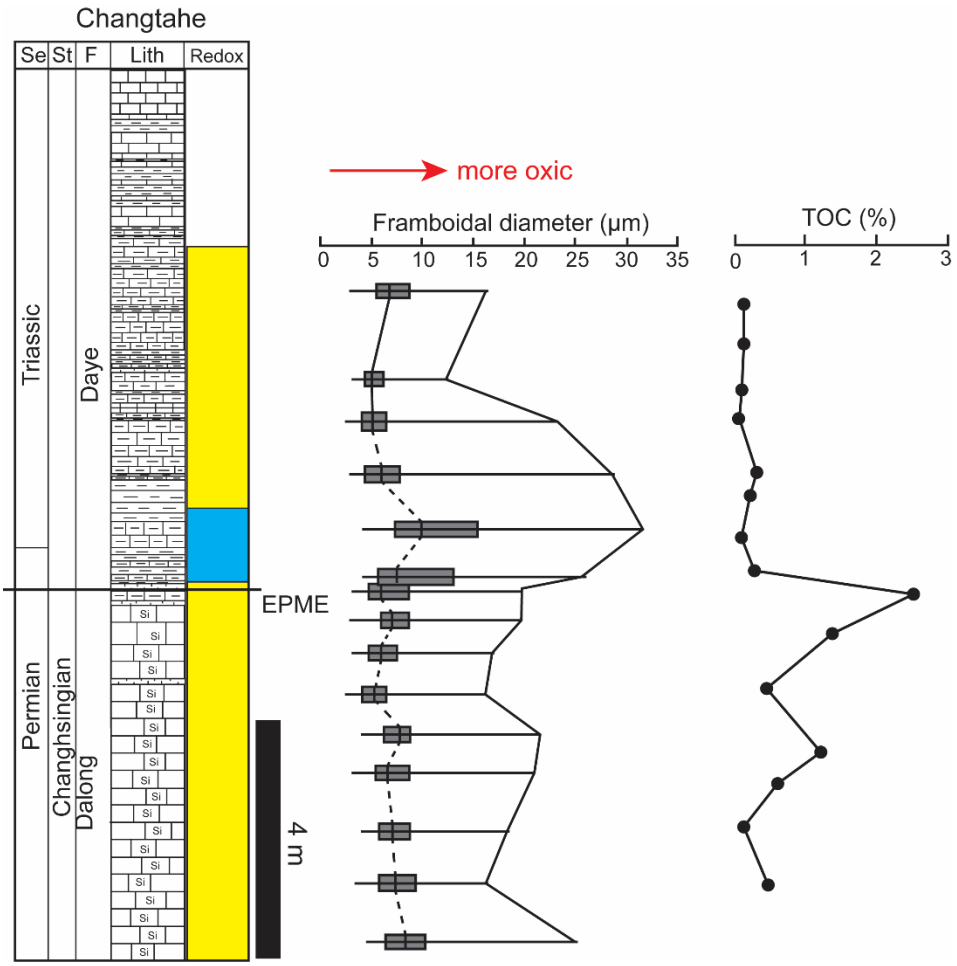

Fig. S5 Lithology, redox and redox-related proxies in the Changtahe section. Details of data and related explanation can be seen in He et al. (2013).

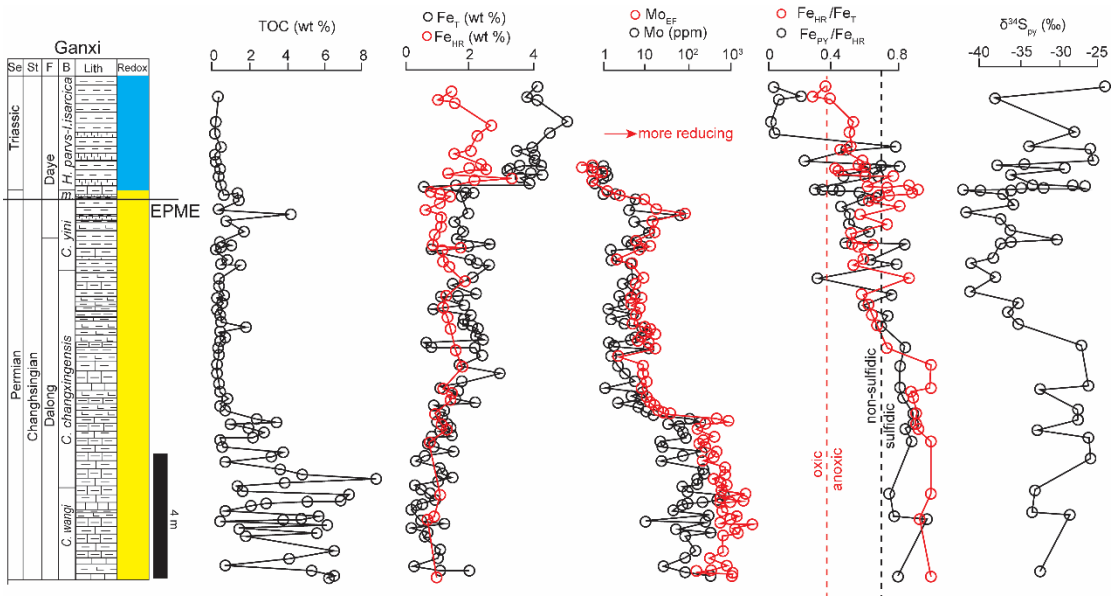

Fig. S6 Lithology, redox and redox-related proxies in the Ganxi section. Details of data and related explanation can be seen in Lei et al. (2017).

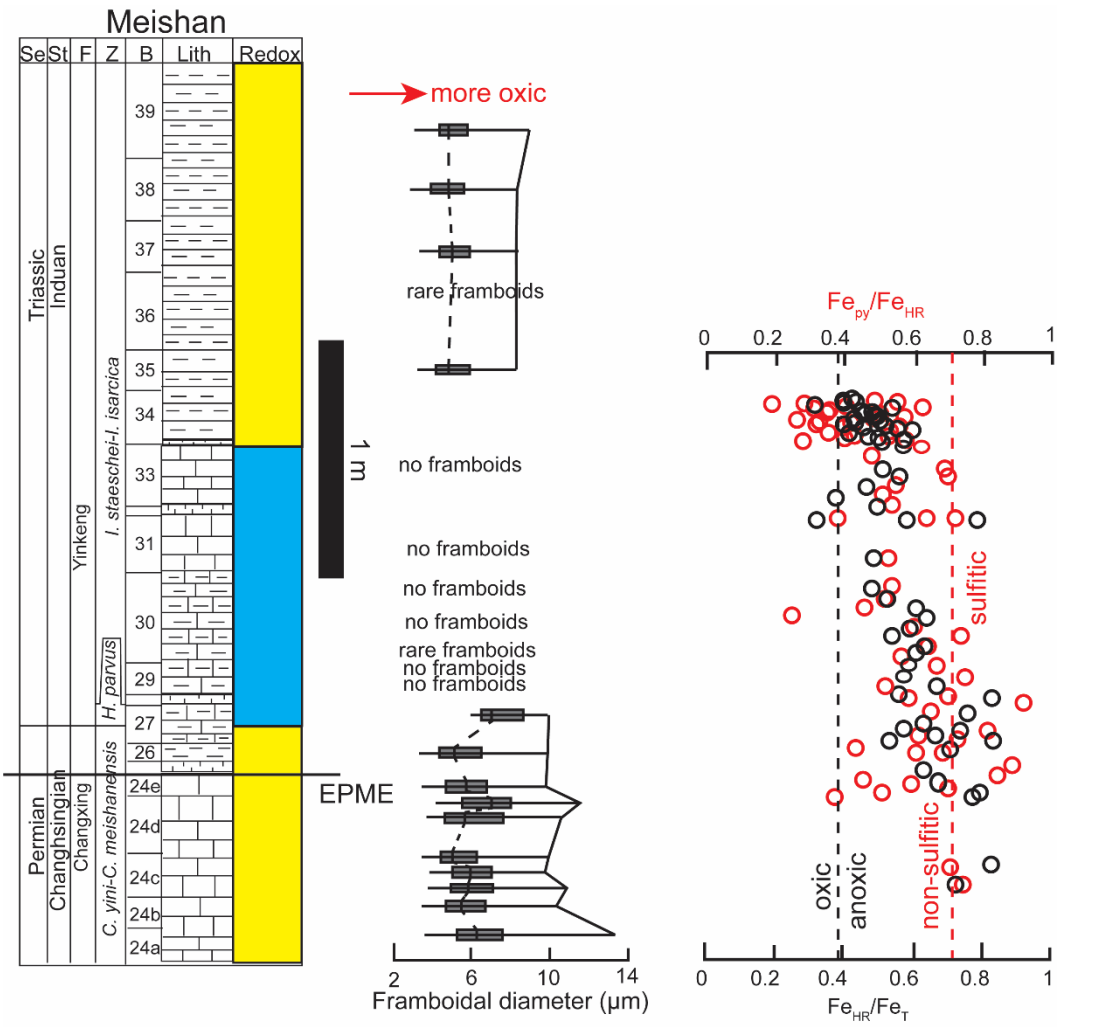

Fig. S7 Lithology, redox and redox-related proxies in the Meishan section. Details of data and

related explanation can be seen in Li et al. (2016) and Xiang et al. (2020).

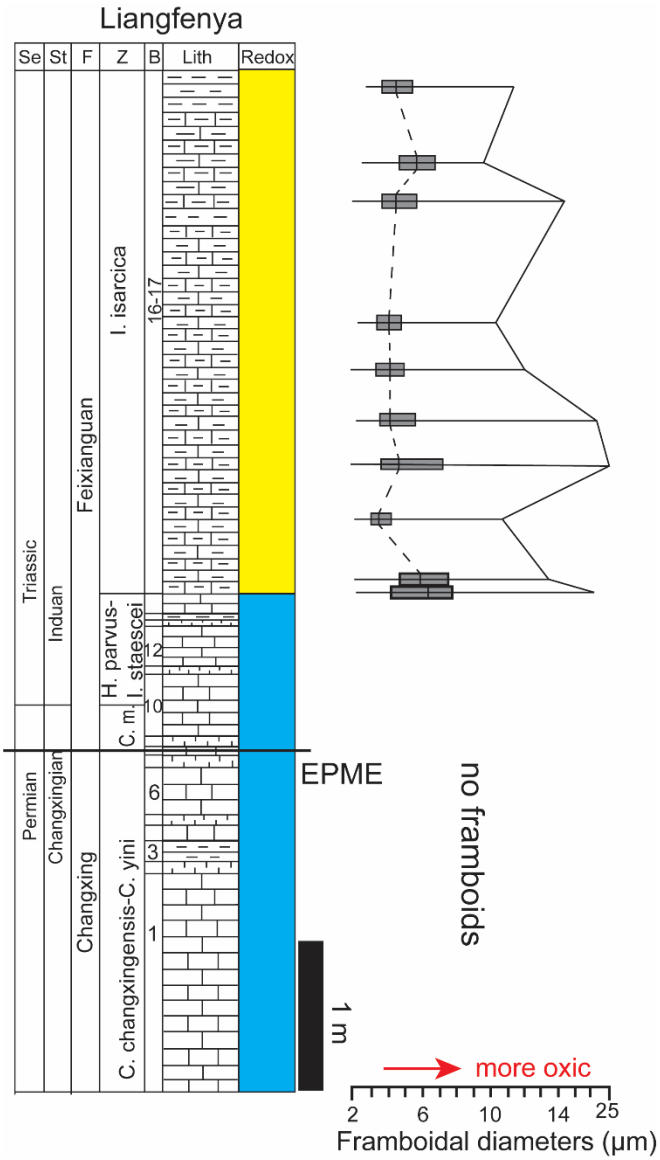

Fig. S8 Lithology, redox and redox-related proxies in the Liangfengya section. Details of data and related explanation can be seen in Li et al. (2021).

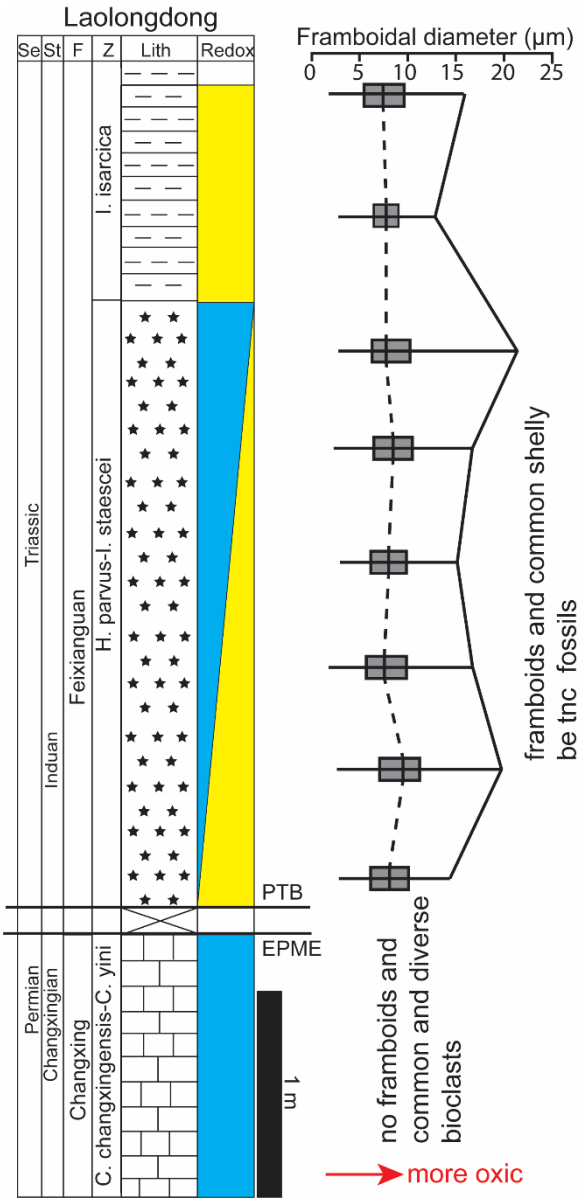

Fig. S9 Lithology, redox and redox-related proxies in the Laolongdong section. Details of data and related explanation can be seen in Liao et al. (2010) and Li et al. (2021).

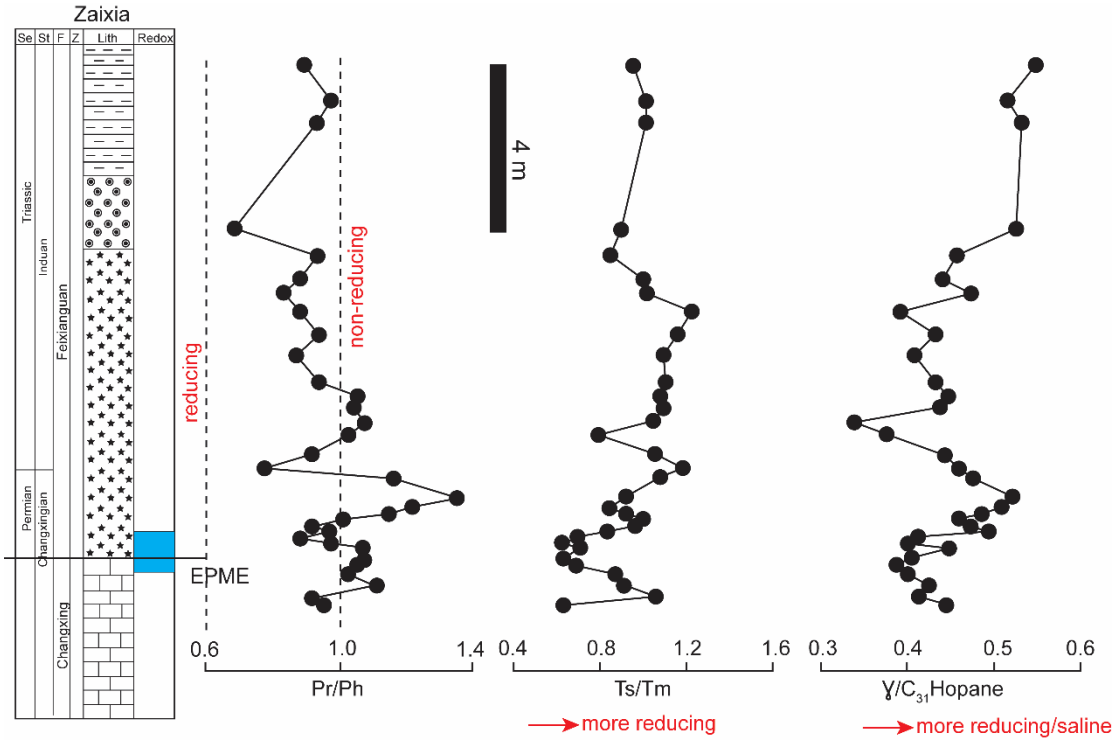

Fig. S10 Lithology, redox and redox-related proxies in the Zaixia section. Details of data and related explanation can be seen in Adachi et al. (2017).

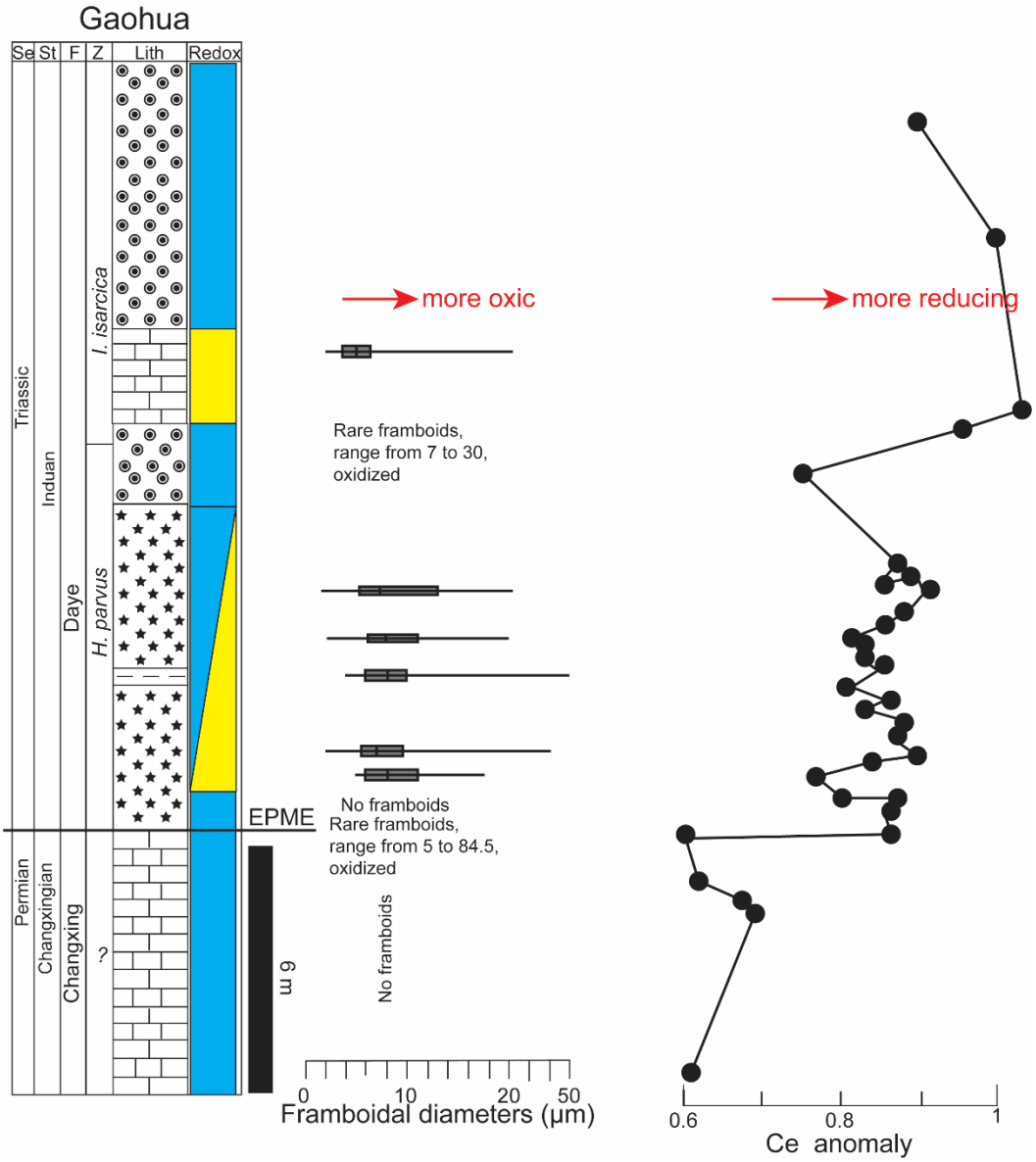

Fig. S11 Lithology, redox and redox-related proxies in the Gaohua section. Details of data and related explanation can be seen in Loope et al. (2013) and Wang et al. (2016).

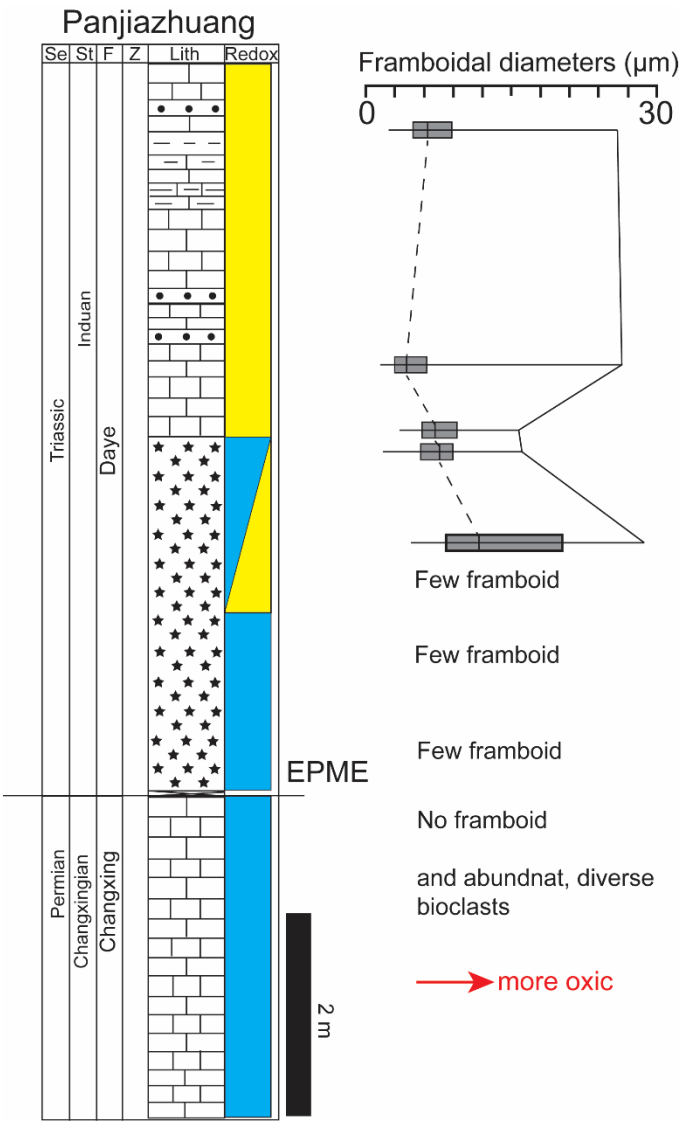

Fig. S12 Lithology, redox and redox-related proxies in the Panjiazhuang section. Details of data and related explanation can be seen in Huang et al. (2019).

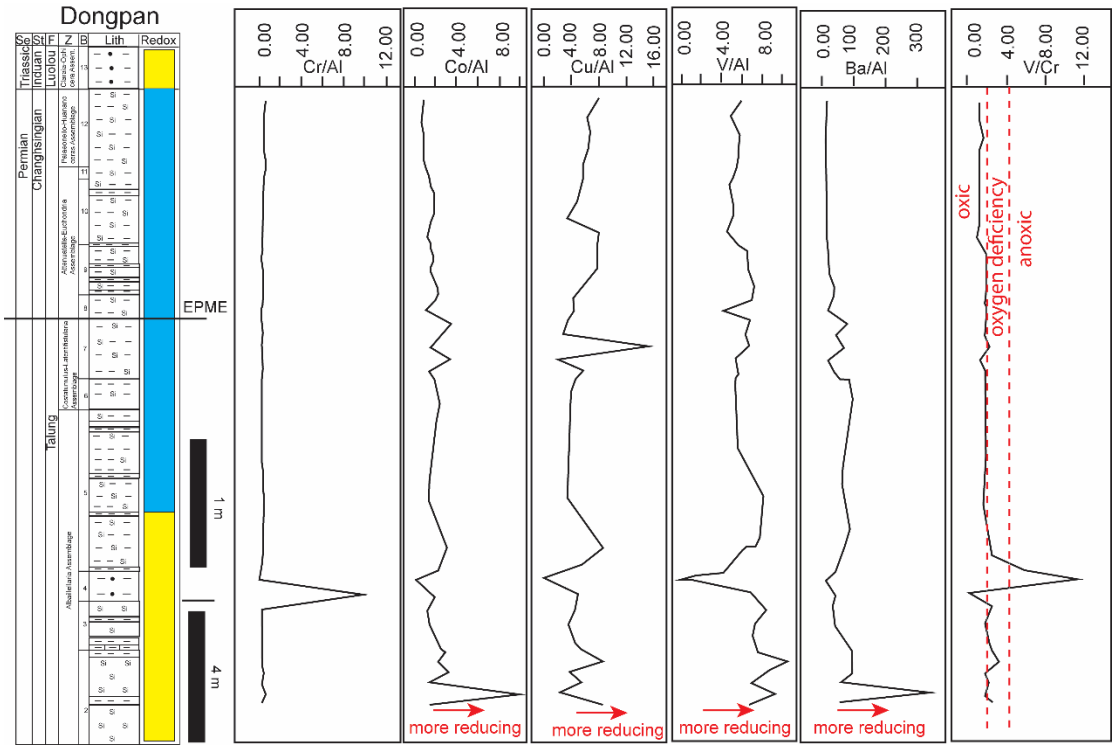

Fig. S13 Lithology, redox and redox-related proxies in the Dongpan section. Details of data and related explanation can be seen in He et al. (2007).

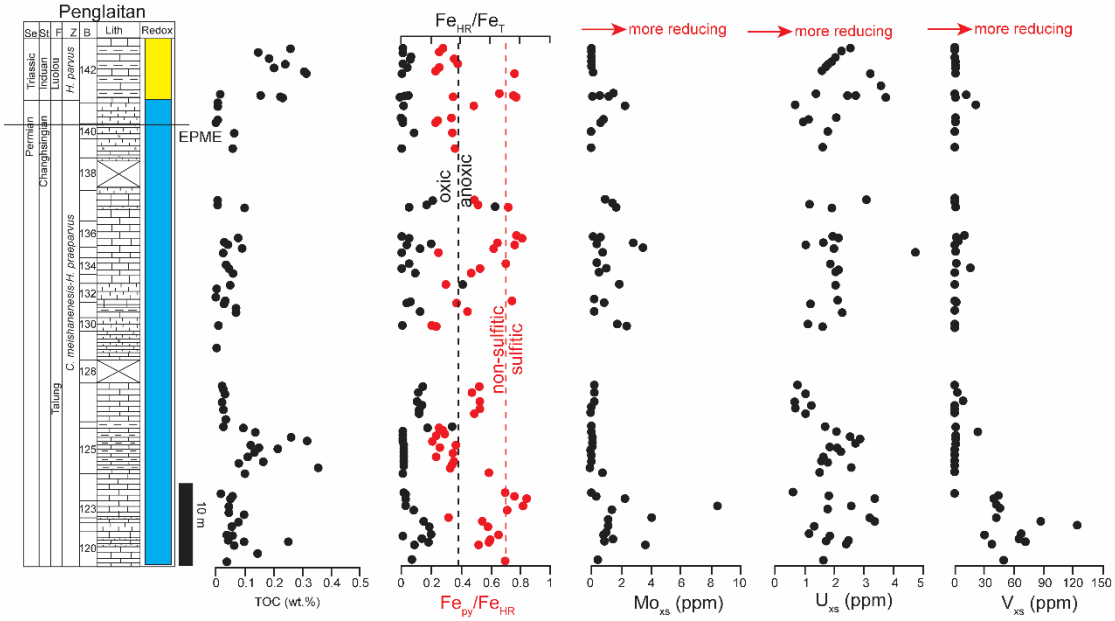

Fig. S14 Lithology, redox and redox-related proxies in the Penglaitan section. Details of data and related explanation can be seen in Xiang et al. (2021).

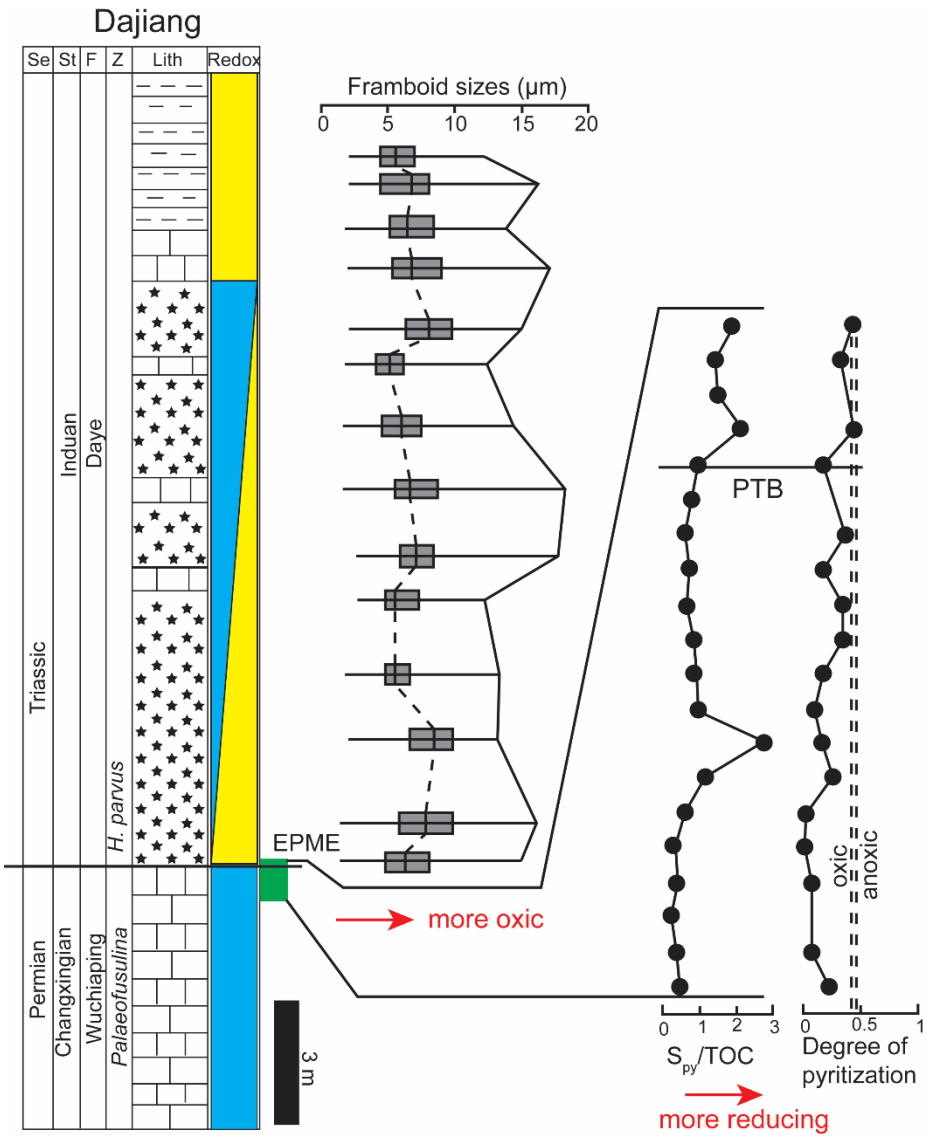

Fig. S15 Lithology, redox and redox-related proxies in the Dajiang section. Details of data and related explanation can be seen in Song et al. (2014) and Liao et al. (2017).

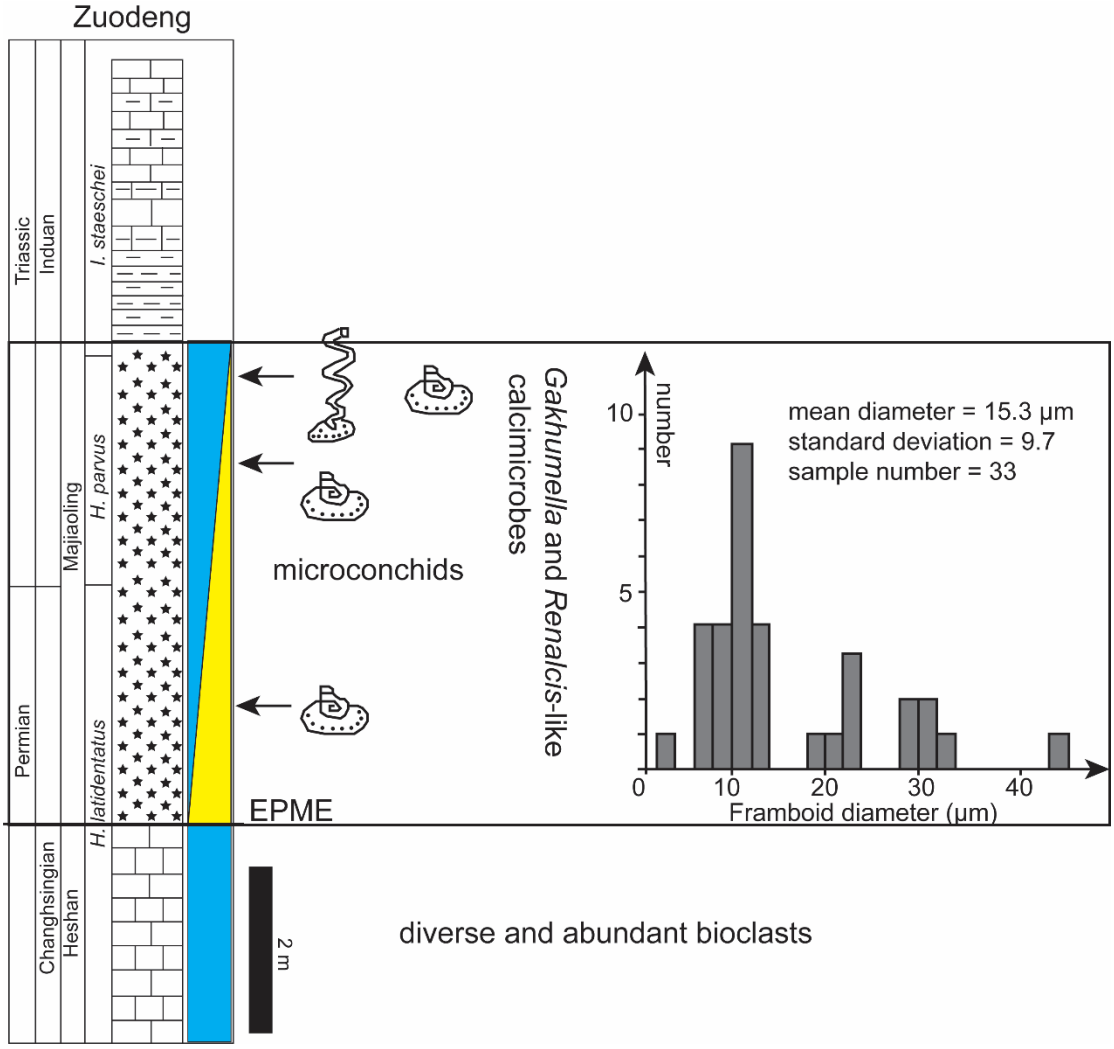

Fig. S16 Lithology, redox and redox-related proxies in the Zuodeng section. Details of data and related explanation can be seen in Yang et al. (2015) and Fang et al. (2017).

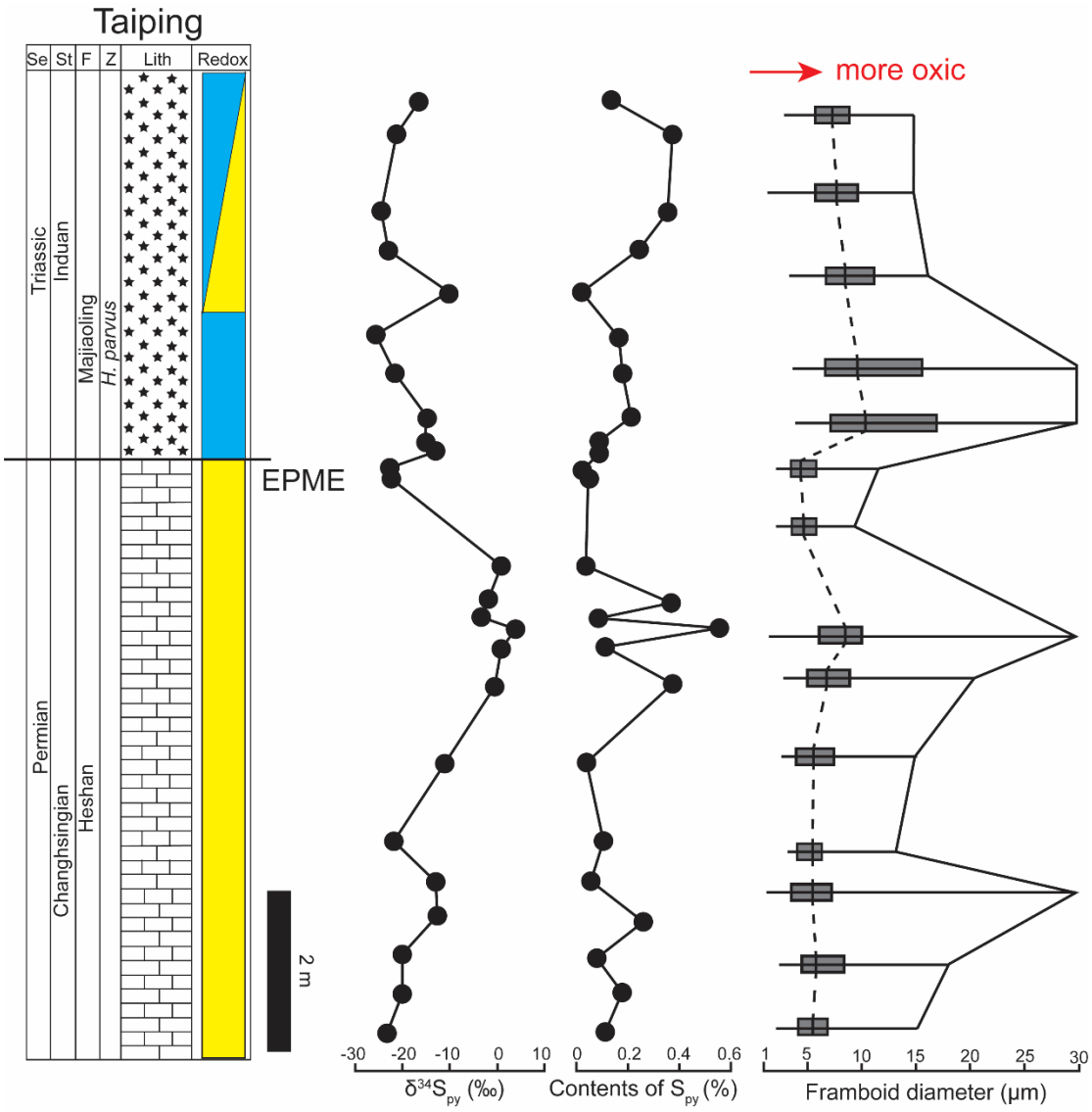

Fig. S17 Lithology, redox and redox-related proxies in the Taiping section. Details of data and related explanation can be seen in Xiao et al. (2018).

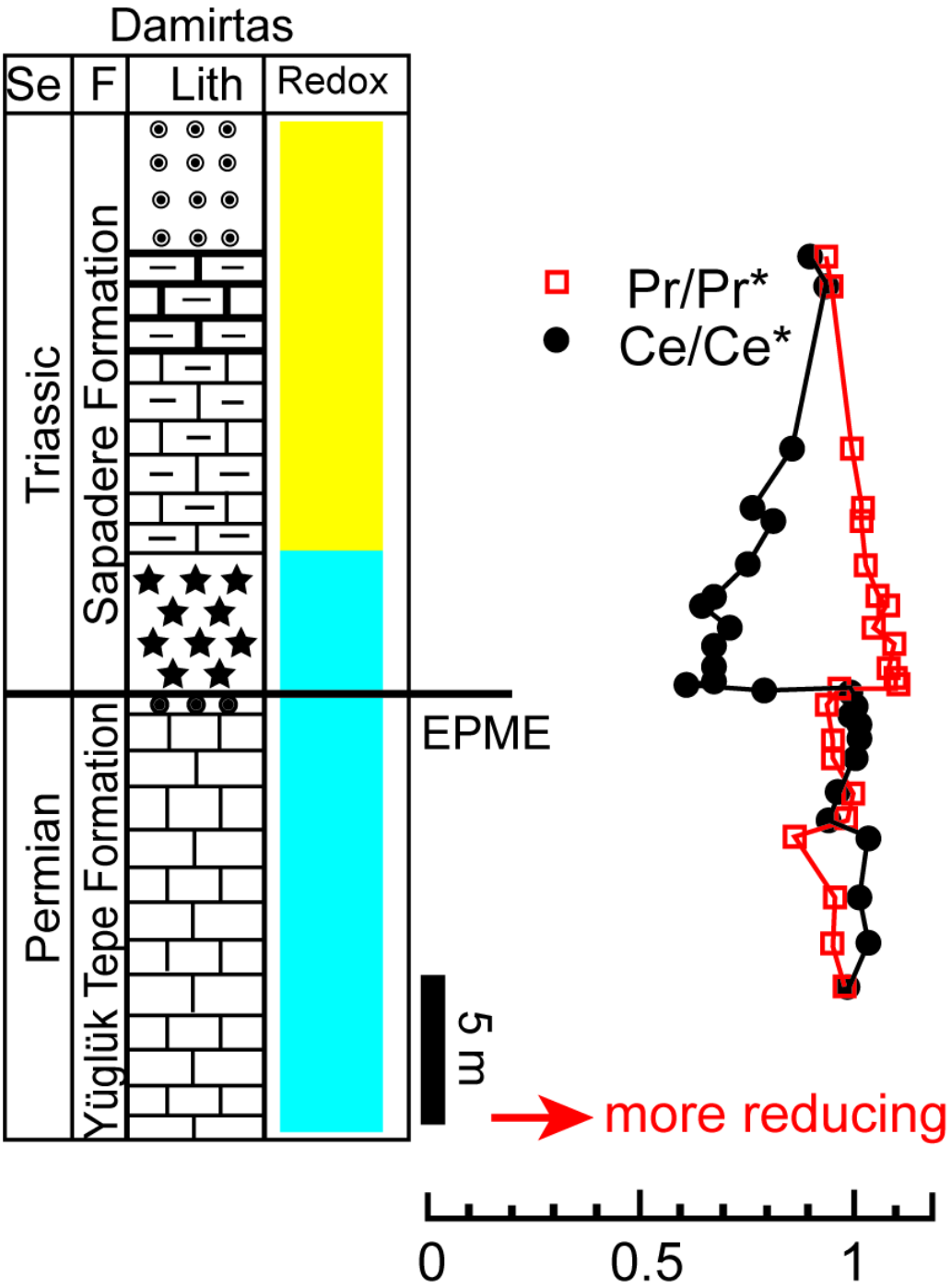

Fig. S18 Lithology, redox and redox-related proxies in the Damirtas section. Details of data and related explanation can be seen in Loope et al. (2013).

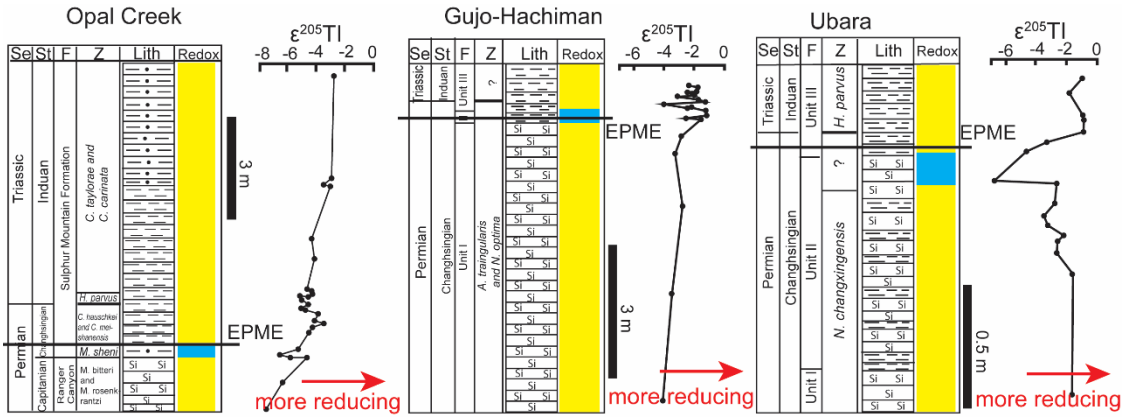

Fig. S19 Lithology, redox and redox-related proxies in the Panthalassic section. Details of data and related explanation can be seen in Newton et al. (2004).